

## Strain weakening and superplasticity in a Bi-Sn eutectic alloy processed by high-pressure torsion

This content has been downloaded from IOPscience. Please scroll down to see the full text.

2014 IOP Conf. Ser.: Mater. Sci. Eng. 63 012107

(<http://iopscience.iop.org/1757-899X/63/1/012107>)

View [the table of contents for this issue](#), or go to the [journal homepage](#) for more

Download details:

IP Address: 152.78.130.228

This content was downloaded on 12/09/2014 at 13:21

Please note that [terms and conditions apply](#).

# Strain weakening and superplasticity in a Bi-Sn eutectic alloy processed by high-pressure torsion

**Chuan Ting Wang<sup>1</sup> and Terence G Langdon<sup>1,2</sup>**

<sup>1</sup>Departments of Aerospace & Mechanical Engineering and Materials Science  
University of Southern California, Los Angeles, CA 90089-1453, U.S.A.

<sup>2</sup>Materials Research Group, Faculty of Engineering and the Environment,  
University of Southampton, Southampton SO17 1BJ, U.K.

E-mail: [chuanting.wang@usc.edu](mailto:chuanting.wang@usc.edu)

**Abstract.** High-pressure torsion (HPT) was conducted on disks of a Bi-Sn eutectic alloy under a pressure of 6.0 GPa. The microstructural evolution was studied by scanning electron microscopy (SEM) and electron backscatter diffraction (EBSD). Measurements of Vickers microhardness showed decreasing strength caused by strain weakening after HPT processing. Tensile testing was performed under initial strain rates from  $10^{-4}$  to  $10^{-2}$  s<sup>-1</sup> at room temperature. The results demonstrate a much improved elongation to failure for the Bi-Sn alloy after HPT-processing. The Bi-Sn alloy processed through 10 turns gave an elongation to failure of more than 1200% at an initial strain rate of  $10^{-4}$  s<sup>-1</sup> at room temperature which is significantly larger than the elongation to failure of ~110% in the as-cast Bi-Sn alloy under the same tensile conditions.

## 1. Introduction

Superplasticity refers to the exceptionally high elongations to failure, normally larger than 400%, that may occur in some metallic alloys under tensile conditions [1]. The first study achieving true superplastic deformation in metals was reported by Pearson in 1934 [2]. In this study, the Bi-Sn eutectic alloy was extruded and aged for 7 days and an impressive elongation to failure of ~1950% was achieved when the sample was tested under a constant stress of ~250 lb·inch<sup>-2</sup> (~1.7 MPa). More recently, remarkable elongations have been reported in numerous metallic alloys including an elongation of 7550% in a Pb-62% Sn eutectic alloy [3].

It is now well recognized that two conditions are required for superplastic flow [4]. First, the testing must be conducted at a high temperature, typically  $\geq 0.5 T_m$  where  $T_m$  is the absolute melting temperature of the metal. Second, the tested material should have a small and stable grain size so that grain boundary sliding can occur easily. Because of these requirements, extensive research has been directed towards achieving superplasticity in metals by refining the grain size.

During the past two decades, much attention has focused on processing metals through the application of severe plastic deformation (SPD) to achieve exceptional grain refinement. A unique feature of SPD processing is that the strain is imposed without any significant change in the overall dimensions of the work-piece. Therefore, it is possible to impose a large strain to the sample by repeating the SPD processing. Much attention has been given to the two SPD processing methods of equal-channel angular pressing (ECAP) [5] and high-pressure torsion (HPT) [6]. Recently, ECAP was conducted on a magnesium ZK60 alloy and an elongation of 3050% was achieved after processing for 2 passes and then testing in tension at 473 K using a strain rate of  $1.0 \times 10^{-4}$  s<sup>-1</sup> [7]. Similarly, a Pb-62% Sn eutectic alloy was processed by ECAP for 16 passes and a superplastic elongation of 3060% was achieved under a strain rate of  $1.0 \times 10^{-3}$  s<sup>-1</sup> at 413 K [8]. In a later study, a Pb-62% Sn alloy containing 160 ppm of Sb was processed by ECAP for 4 passes and this gave an elongation of 2665% under a



strain rate of  $1.0 \times 10^{-4} \text{ s}^{-1}$  at 423 K [9]. Although these results refer to samples processed by ECAP, there is also a report of a superplastic elongation of 1800% in a Zn-22% Al eutectoid alloy after processing by HPT for 5 turns at room temperature and then pulling to failure at 473 K at a rapid strain rate of  $1.0 \times 10^{-1} \text{ s}^{-1}$  [10]. All of these results demonstrate that SPD processing provides a capability for achieving exceptional superplastic ductilities and these very high elongations are especially associated with two-phase eutectic and eutectoid alloys. Although much of the attention to date has been devoted to the Pb-62% Sn alloy, it is interesting to note that the Bi-Sn eutectic alloy is important as a lead-free low-temperature solder and, in addition, this alloy is of interest as a model metal to study superplastic flow at room temperature [11].

Accordingly, the present investigation was initiated as the first study on HPT processing of the Bi-Sn alloy. Thus, the present tests were undertaken with two specific objectives. Firstly, to investigate the grain refinement and mechanical property evolution after HPT processing with special attention devoted to the thermal stability of the microstructure at room temperature. Secondly, to determine the optimum testing conditions in order to achieve superplastic ductilities during tensile testing.

## 2. Experimental procedures

The Bi-42% Sn eutectic alloy was supplied as a cast ingot with approximate dimensions of  $55 \times 35 \times 250 \text{ mm}^3$ . Thin disk samples with diameters of 10 mm were machined from the cast ingot and these disks were then carefully ground to give disk thicknesses between 0.80 and 0.85 mm. No heat treatment was performed on the alloy before HPT processing because the alloy has a very low melting temperature of 411 K. Therefore, this alloy will experience self-annealing when held at room temperature of 298 K.

The HPT processing was conducted under quasi-constrained conditions where there was some restricted outflow of material around the periphery of the sample during the processing operation [12,13]. The HPT facility consisted of massive upper and lower anvils that were arranged in a vertical alignment. Each anvil had a circular depression on the inner face with a diameter of 10 mm and a depth of 0.25 mm. For HPT processing, a disk was placed in the depression on the lower anvil, the lower anvil was then raised to hold the disk between the two anvils, a pressure of 6.0 GPa was imposed on the disk and then torsional straining was generated by rotation of the lower anvil. Various total strains were imposed on the disks by processing for 1, 5 or 10 revolutions at a constant rotation speed of 1 rpm.

After HPT processing, disks of both the as-cast and the HPT-processed Bi-Sn alloy were polished by abrasive papers to 1600 grit followed by polishing to  $1 \mu\text{m}$  with diamond suspensions. Finally, vibratory polishing was performed with a  $0.04 \mu\text{m}$  colloidal silica suspension to remove any scratches. A solution of 25 ml  $\text{H}_2\text{O}$ , 5 ml  $\text{HCl}$  with a concentration of 37 % and 5 g of  $\text{NH}_4\text{NO}_3$  was used as the etchant. The microstructure was observed using a scanning electron microscope (SEM) JEOL JSM-7001 F at an operating voltage of 15 kV. The SEM was equipped with an electron backscatter diffraction (EBSD) detector and used a TSL orientation imaging system and OIM™ software to analyze the results. The EBSD data were collected at a working distance of 15 mm with a sample tilt of  $70^\circ$ .

Microhardness measurements were taken on the polished surfaces using an FM-1e Vickers hardness tester using a load of 50 gf with a dwell time of 10 s for each individual indentation. Due to the limited size of the HPT disks, two miniature tensile specimens with gauge lengths of 1 mm were machined from off-center positions in the HPT disks according to the procedure described earlier [14]. A special sample holder was designed to fit the tensile sample within the testing machine. These specimens were tested in tension using an Instron facility at room temperature operating under conditions of constant cross-head displacement with initial strain rates from  $1.0 \times 10^{-4}$  to  $1.0 \times 10^{-2} \text{ s}^{-1}$ .

### 3. Experimental results and discussion

#### 3.1. Microstructure of as-cast Bi-42% Sn alloy

Figure 1 shows an SEM image of the as-cast Bi-Sn alloy. It is apparent that the alloy has a lamellar structure and the two phases have area ratios of about 6:4. The darker phase in the SEM image is Bi and the lighter phase is Sn. Since the etchant was attacking the Sn phase, the Bi phase tends to remain as islands. Many fine Bi particles were also observed within the Sn-rich phase. Some pitting holes were observed in the Bi-rich phase which remained because Sn particles were etched away by the etchant. Nevertheless, the number of Sn particles within the Bi phase was significantly smaller than the number of Bi particles within the Sn phase.

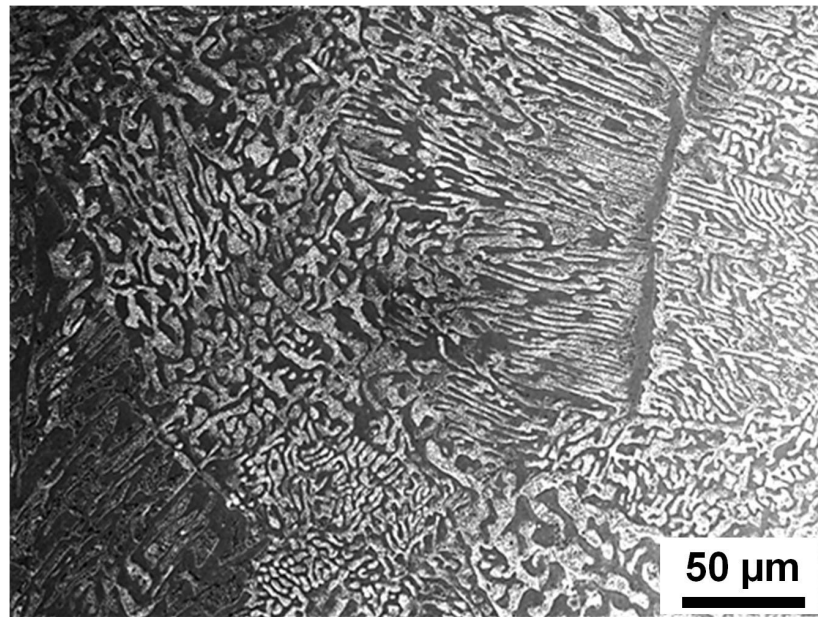


Fig 1 Microstructure of as-cast Bi-Sn.

#### 3.2. Thermal stability of UFG structure and properties

Due to its low melting temperature of 411 K, it is reasonable to anticipate that the UFG structure obtained via HPT processing will be unstable at room temperature. Figure 2 shows the microstructures of the Bi-Sn alloy after HPT processing for (a,b) 1 turn, (c, d) 5 turns and (e, f) 10 turns and then aged at room temperature for (a, c, e) 7 days and (b, d, f) 35 days. It is readily concluded that self-annealing plays a significant role in this material.

In processing by HPT, the shear strain,  $\gamma$ , at different positions on the disk is proportional to the distance from the center of the disk through a relationship of the form [15]:

$$\gamma = \frac{2\pi Nr}{h} \quad (1)$$

where  $N$  is the number of rotation revolutions,  $r$  is the distance from the center of the disk and  $h$  is the height (or thickness) of the sample. Because of this variation in strain, all of the images in Fig 2 were taken at positions which were approximately 2 mm from the center of each disk.

There are several significant features of the microstructures shown in Fig 2. Firstly, processing by HPT leads to a breaking of both of the two phases. As shown in Fig 1, the as-

cast alloy had individual phases having continues band-like shapes After HPT processing for 1 turn these bands were starting to become discontinuous in Fig. 2(a) and after 10 turns in Fig. 2(e) the phases were similar to islands with equiaxed shapes. Secondly, it is apparent from a comparison of Fig. 2(a,c,e) and Fig. 2(b,d,f) that the separate phases are gradually returning during the self-annealing operation.

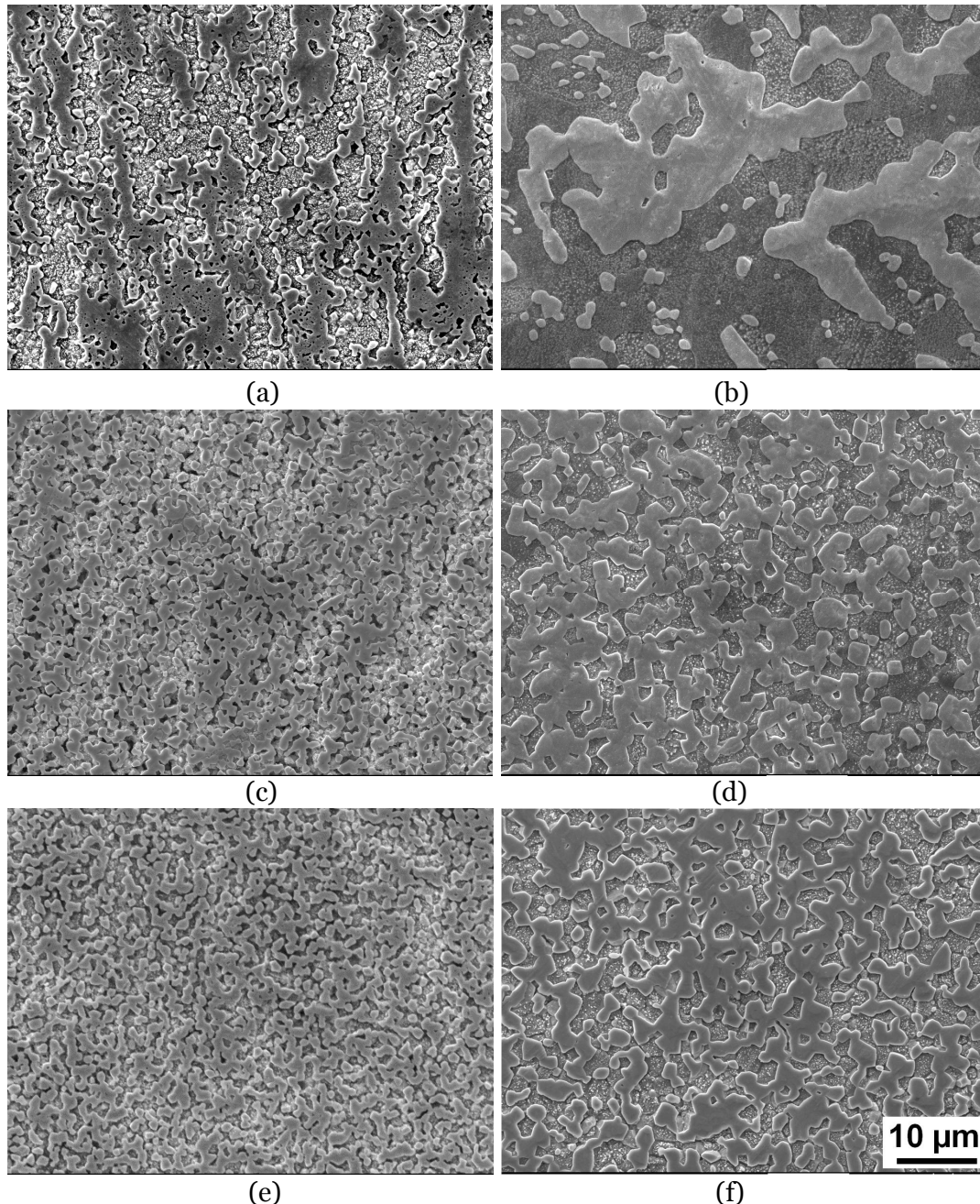


Fig 2 Microstructure Bi-42% Sn after HPT-processing for 1 (a, b), 5 (c, d) and 10 (e, f) revolutions and aged at room temperature for 7 (a, c, e) and 35 (b, d, f) days.

To obtain a better understanding of this effect, a sample processed through 5 turns was selected to track the recovery of the Bi-Sn alloy after HPT processing. Ten individual hardness

measurements were taken at 2 mm from the center of the sample and these microhardness values were plotted against the ageing time at room temperature as shown in Fig 3. Thus, the average hardness of Bi-Sn decreased from 25.4 Hv for the as-cast state as shown by the upper dashed line in Fig. 3 to a value of  $8.4 \pm 0.7$  Hv after 5 turns of HPT and thereafter it increased rapidly to  $16.1 \pm 0.7$  Hv after ageing at room temperature for 1 day. Later, the hardness increased at a slower rate to  $21.2 \pm 0.7$  Hv after ageing for 21 days and then to  $22.3 \pm 0.6$  Hv after ageing for 70 days. Table 1 summarizes measured values for the phase spacing and the microhardness values for the as-cast condition and after ageing for 7 and 35 days.

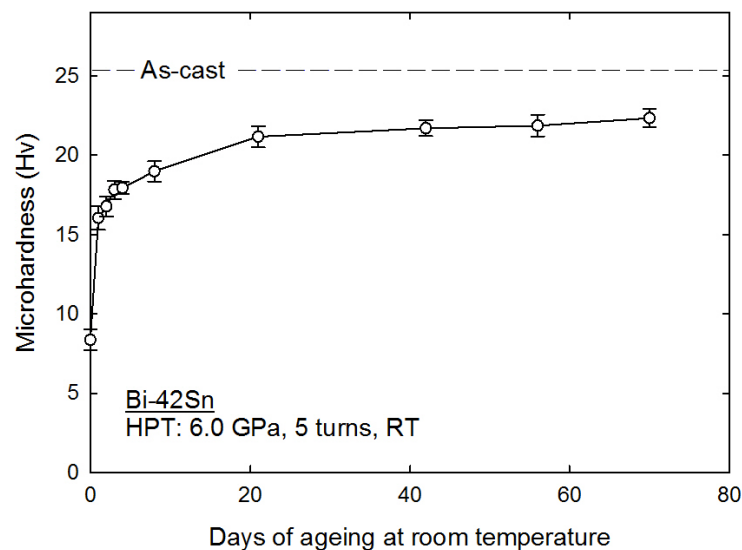


Fig 3 Microhardness of 5 turns HPT processed Bi-Sn versus number of days ageing at room temperature.

Table 1 Phase spacing and microhardness of Bi-Sn alloy

Sample	Phase spacing, $\mu\text{m}$	Microhardness, Hv
As-cast	$3.5 \pm 0.7$	25.4
5 turns+aged 35 days	$2.3 \pm 0.2$	$21.7 \pm 0.5$
5 turns+aged 7 days	$1.0 \pm 0.2$	$19.0 \pm 0.6$

Processing by HPT is one of the most developed SPD methods and it has been used extensively to produce UFG microstructures for a wide range of metals. For many of these materials, results are available showing the variations of hardness across disk diameters after processing by HPT. A recent review provided a comprehensive summary of all of the results available to date [16]. For almost all metals, the HPT processing reduces the grain size and at the same time produces values for the microhardness which are higher than in the initial alloy before HPT processing. These increases in the microhardness denote a hardening effect which generally occurs without any associated recovery but may occur, as in high purity aluminum [17], with some local recovery because of the high stacking fault energy which leads to the easy and rapid cross-slip of dislocations. In the earlier review [16], there were only two exceptions to this trend of hardening by HPT and these exceptions occurred for the Zn-22% Al eutectoid alloy and the Pb-62% Sn eutectic alloy. Thus, although both of these alloys were successfully processed by HPT to give significant grain refinement, microhardness measurements showed a decrease in hardness rather than an increase due to the application of torsional straining. Several sets of data are now available showing this



effect for both the Zn-22% Al alloy [18-20] and the Pb-62% Sn alloy [20]. These results demonstrate the possibility of a strain weakening effect in some two-phase alloys although weakening was not observed in the Al-33% Cu eutectic alloy [21]. The strain weakening effect by HPT processing of the Zn-22% Al alloy was attributed to the loss of rod-shaped Zn precipitates within the Al-rich grains because earlier observations by transmission electron microscopy demonstrated that the high pressures associated with HPT processing led to an absorption of the Zn particles by the Zn-rich grains [22].

To check for a similar possibility in the Bi-Sn alloy, a disk was processed by HPT for 10 turns and then aged at room temperature for 35 days. Figure 4 shows the phase distribution diagram generated from the EBSD data where the Bi phase is red and the Sn phase is green. It is clear that after HPT processing for 10 turns both the Bi and Sn precipitates are visible within the other phase thereby suggesting that the absorption of precipitates is not so important in the Bi-Sn alloy during HPT processing. More research will be needed to fully identify the origin of the strain weakening effect in the Bi-Sn alloy.

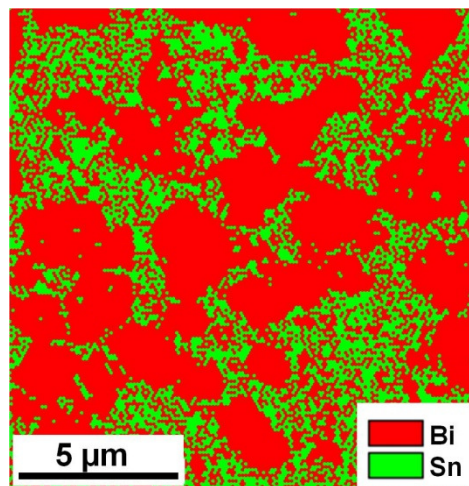


Fig 4 Phase distribution diagram of Bi-Sn alloy processed by HPT for 10 turns and aged at room temperature for 35 days.

During HPT processing, the phases are generally broken up, the phase spacing is reduced and the microhardness is also reduced. During the self-annealing process at room temperature, both phases tend to grow together again thereby producing increases in both the phase spacing and the hardness. Relevant measurements showing this effect are given in Table 1. It seems from these measurements that the Bi-Sn phase boundary is weak and therefore samples with more Bi-Sn boundaries, and therefore smaller phase spacing, have lower values for the hardness.

### 3.3. Tensile properties of the Bi-42% Sn alloy

As shown in Fig 3, the self-annealing becomes very slow after ageing for about 21 days. Therefore, tensile testing of the HPT-processed Bi-Sn alloy was performed after ageing for 35 days so that it is reasonable to neglect the effect of any self-annealing of the alloy during the tensile testing. Tensile samples were pulled to failure at room temperature (298 K) under initial strain rates of  $1.0 \times 10^{-2}$ ,  $1.0 \times 10^{-3}$  and  $1.0 \times 10^{-4} \text{ s}^{-1}$ . Figure 5(a) shows the true stress-true strain curves for different samples under an initial strain rate of  $1.0 \times 10^{-2} \text{ s}^{-1}$ . Thus, the as-cast sample has the highest flow stress of  $\sim 58 \text{ MPa}$  but the lowest elongation to failure of  $\sim 54\%$ . By contrast, the sample processed through 10 turns of HPT has a lower flow stress of  $\sim 35 \text{ MPa}$  but an elongation to failure of  $\sim 200\%$ . Figure 5 (b) shows a similar set of stress-strain curves for samples processed by HPT for 5 turns, aged at room temperature for 35

days and then tested in tension at different strain rates at room temperature. It is readily apparent from this plot that slower strain rates lead to higher elongations to failure and also to lower flow stresses.

To provide a comprehensive summary of the results, the elongations to failure of each sample aged for 35 days and then tested under different initial strain rates is documented in Fig. 6. The results show that the as-cast Bi-Sn alloy has only very limited ductility when testing at strain rates from  $10^{-4}$  to  $10^{-2} \text{ s}^{-1}$  with measured elongations that are  $<200\%$  although with a tendency for a higher elongation at the slowest strain rate. Processing by HPT leads to a very significant increase in the measured ductilities at all strain rates. For example, using an initial strain rate of  $1.0 \times 10^{-4} \text{ s}^{-1}$ , processing by 10 turns of HPT produced a sample with an elongation to failure of  $\sim 1200\%$  which is an improvement of more than ten times compared with the elongation to failure of  $\sim 110\%$  recorded in the as-cast and unprocessed alloy when testing at the same strain rate. In the very early study by Pearson [2], the Bi-Sn alloy was extruded and aged for 7 days and then exhibited an elongation to failure of  $\sim 1950\%$ . This elongation is significantly larger than in the present experiments but it is important to note that the earlier tests were conducted using relatively large cylindrical samples whereas in the present investigation the tensile tests were conducted using miniature dog-bone samples that were cut directly from the HPT disks after processing. The lower elongations in the present study are a direct consequence of the use of small specimens with very thin cross-sections. It was shown in earlier studies that care must be exercised in interpreting tensile data from miniature samples because the lower values for the elongations to failure are a direct consequence of the gauge lengths and the very small cross-sectional areas [23,24]. It is important to note also that the sample used by Pearson was tested under creep conditions with a constant load of  $\sim 250 \text{ lb-inch}^{-2}$  equivalent to  $\sim 1.7 \text{ MPa}$  [2] whereas in the present investigation the samples were pulled to failure in a testing facility operating at a constant rate of cross-head displacement.

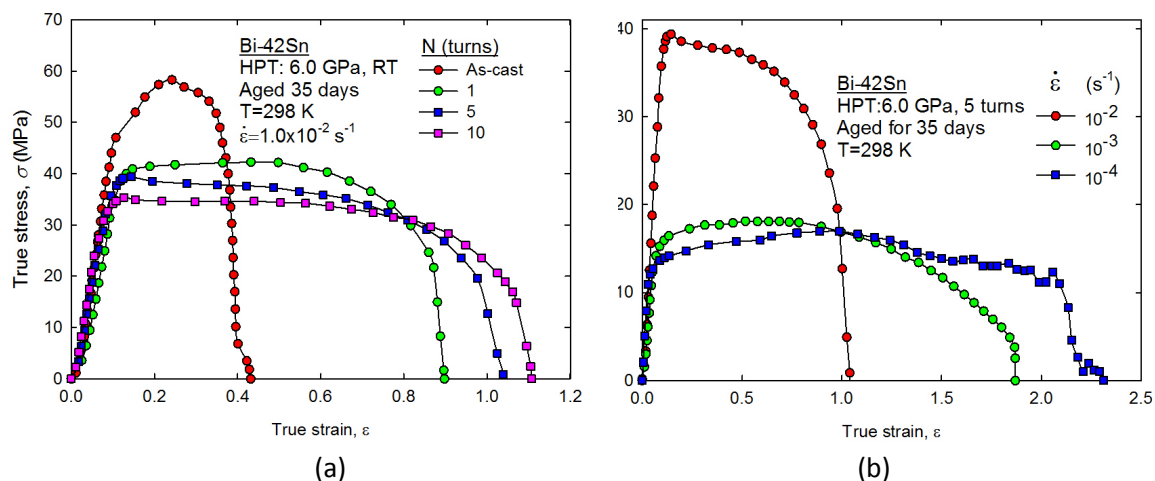


Fig 5 True stress-true strain curves of Bi-Sn alloy after ageing for 35 days,  
 (a) different samples under same strain rate of  $1.0 \times 10^{-2} \text{ s}^{-1}$ ;  
 (b) 5 turns deformed samples under different strain rates.



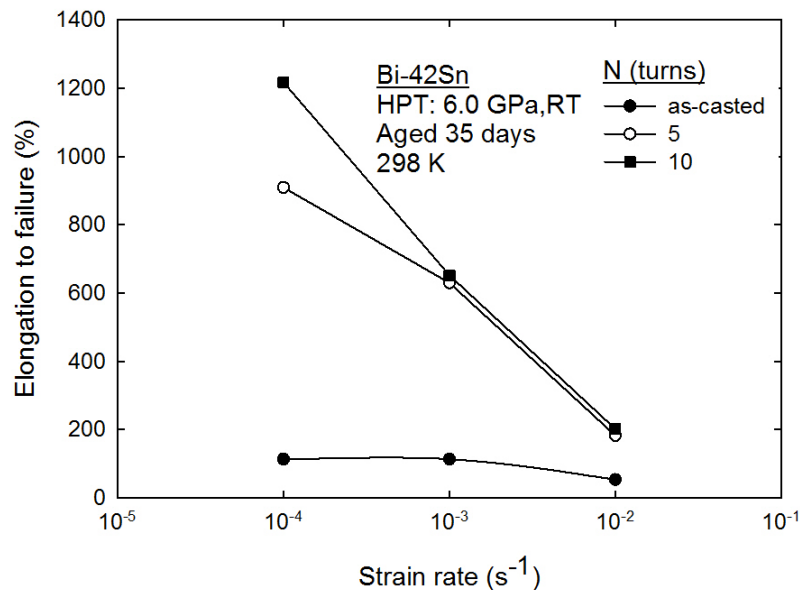


Fig 6 Variation of the elongation to failure versus the initial strain rate for samples processed various turns of HPT and pulled at room temperature.

#### 4. Summary

1. A Bi-42% Sn eutectic alloy was successfully processed by HPT. After processing, there was a strain weakening and a decrease in the phase spacing and the microhardness.
2. Self-annealing occurred during storage at room temperature. The phase spacing and the microhardness both increased with increasing time of storage.
3. Processing by HPT significantly improved the ductility of the Bi-Sn alloy in tensile testing at room temperature. A superplastic elongation of ~1200% was achieved after processing by HPT through 10 turns and pulling to failure at an initial strain rate of  $1.0 \times 10^{-4} \text{ s}^{-1}$ .

#### Acknowledgements

This work was supported in part by the National Science Foundation of the United States under Grant No. DMR-1160966 and in part by the European Research Council under ERC Grant Agreement No. 267464-SPDMETALS.

#### References

- [1] Langdon T G 2009 *J. Mater. Sci.* **44** 5998
- [2] Pearson C E 1934 *J. Inst. Metals* **54** 111
- [3] Ma Y and Langdon T G 1994 *Metall. Mater. Trans. A* **25** 2309
- [4] Langdon T G 1982 *Metall. Trans. A* **13** 689
- [5] Valiev R Z and Langdon T G 2006 *Prog. Mater. Sci.* **51** 881
- [6] Zhilyaev A P and Langdon T G 2008 *Prog. Mater. Sci.* **53** 893
- [7] Figueiredo R B and Langdon T G 2008 *Adv. Eng. Mater.* **10** 37
- [8] Kawasaki M, Lee S and Langdon T G 2009 *Scripta. Mater.* **61** 963
- [9] Kawasaki M, Mendes A A, Sordi V L, Ferrante M and Langdon T G 2011 *J. Mater. Sci.* **46** 155
- [10] Kawasaki M and Langdon T G 2011 *Mater. Sci. Eng. A* **528** 6140
- [11] Alkorta J and Gil Sevillano J 2004 *J. Mater. Res.* **19** 282
- [12] Figueiredo R B, Cetlin P R and Langdon T G 2011 *Mater. Sci. Eng. A* **528** 8198
- [13] Figueiredo R B, Pereira P H R, Aguilar M T P, Cetlin P R and Langdon T G 2012 *Acta Mater.* **60** 3190

- [14] Loucif A, Figueiredo RB, Kawasaki M, Baudin T, Brisset F, Chemam R and Langdon TG 2012 *J. Mater. Sci.* **47** 7815
- [15] Valiev R Z, Ivanisenko Yu V, Rauch E F and Baudelet B 1996 *Acta Mater.* **44** 4705
- [16] Kawasaki M 2014 *J. Mater. Sci.* **49** 18
- [17] Xu C, Horita Z and Langdon TG 2007 *Acta Mater.* **55** 203
- [18] Kawasaki M, Ahn B and Langdon TG 2010 *Acta Mater.* **58** 919
- [19] Kawasaki M, Ahn B and Langdon TG 2010 *Mater. Sci. Eng. A* **527** 7008
- [20] Zhang N, Kawasaki M, Huang Y and Langdon T G 2013 *J. Mater. Sci.* **48** 4582
- [21] Kawasaki M, Foissey J and Langdon TG 2013 *Mater. Sci. Eng. A* **561** 118
- [22] Furukawa M, Horita Z, Nemoto M, Valiev R Z and Langdon T G 1996 *J. Mater. Res.* **11** 2128
- [23] Zhao Y H, Guo Y Z, Wei Q, Dangelewicz A M, Xu C, Zhu Y T, Langdon T G, Zhou Y Z and Lavernia E J 2008 *Scripta Mater.* **59** 627
- [24] Zhao YH, Guo YZ, Wei Q, Topping TD, Dangelewicz AM, Zhu YT, Langdon TG and Lavernia EJ 2009 *Mater. Sci. Eng. A* **525** 68